Maple in discretizing equations by the Finite Volume Element method

D. Canright
Mathematics Dept., Code MA/Ca
Naval Postgraduate School
Monterey, CA 93943

February 24, 1996

Abstract

The Finite Volume Element (FVE) method combines the exact conservation of finite volumes with the continuous representation of finite elements. One drawback of this approach is that to evaluate the coefficients in the equations (the "stencils"), many simple integrals involving unknowns must be evaluated. This problem is compounded when working with systems of differential equations involving several different operators and/or variable coefficients. This talk will examine one such project, for which *Maple* was used to perform the integrals and much of the algebra in the calculation of the stencils.

1 INTRODUCTION

In ongoing research we are investigating flow in a weld pool, where the temperature variations along the free surface of the liquid metal pool cause differences of surface tension that drive the flow. These thermocapillary effects would be dominant in laser welding, for example. For arc welding the electromagnetic forces predominate, but even there the thermocapillary forces are dominant near the edge of the pool, because of the "positive feedback" between the temperature gradient driving the flow and the flow compressing the thermal gradient [2]. Previous work [1] analyzed this feedback mechanism by isolating the "cold corner" region where the liquid free surface meets the solid as a model problem.

The current research considers a more realistic model for the whole pool. Here the global heat transfer problem is considered, which is coupled to the flow in the liquid, to investigate how the thermocapillary feedback mechanism affects the shape of the solid-liquid interface bounding the pool. This process is modeled computationally, and the steady solution sought for a wide range of the two governing parameters.

The choice of numerical methods was motivated by the requirements of this problem. The heat balance is very important both in driving the flow and in determining the shape of the liquid region, so we wanted a method that exactly satisfies conservation laws. Also, because small local length scales are important along the pool boundary, which is to be determined in the solution, an adaptive grid was required. The Finite-Volume-Element (FVE) discretization was chosen, which combined the exact conservation of Finite Volumes with the continuous representation of Finite Elements. The FVE approach is also well suited to our chosen solver, the Fast Adaptive Composite-Grid (FAC) method for multilevel solution with local refinement.

Implementing this approach on our system of coupled partial differential equations in axisymmetric geometry necessitated the evaluation of a large number of integrals, to find the coefficients ("stencil") for each discrete operator. *Maple* was used to compute these stencils, which not only saved a great deal of tedious effort, but also assured accurate results. Without the automation of stencil calculation through *Maple*, the FVE discretization would have been far less feasible for this complicated problem.

2 PROBLEM STATEMENT

A half-space of a pure material is subjected to concentrated heating on the flat horizontal surface, giving a pool of molten material surrounded by solid. The total heat flux Q is constant, and far away the solid

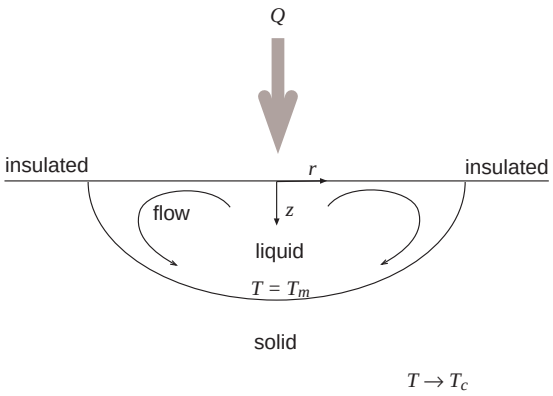

Figure 1: Problem Formulation: a half-space of pure material is subjected to concentrated surface heating Q that results in a molten pool. (Outside the surface heating, the surface is adiabatic.) The melting temperature is T_m, and far away the solid is at the cooler temperature T_c. The flat liquid surface is subject to thermocapillary forcing, which drives convection in the liquid. Axisymmetry is assumed.

approaches the uniform cold temperature T_c (see Figure 1). Above the horizontal free surface is an inviscid, nonconducting gas. Surface tension of the liquid is assumed strong enough to keep the free surface flat (small Capillary number), but with surface tension variations due to a linear dependence on temperature. The resulting thermal and flow fields are assumed to be axisymmetric and steady, but the time-dependent equations are given below, to facilitate a numerical approach using time-like iterations to reach the steady solution.

Then the system is governed by conservation of energy in the solid and by conservation of energy, momentum, and mass in the pool. For the numerical solutions, the equations are suitably nondimensionalized, and a stream-function/vorticity formulation is used for the flow. Then the complete system of dimensionless equations is:

$$\text{solid:} \qquad \frac{\partial T}{\partial t} = Ma^{-1}\,\nabla\cdot\nabla\,T \tag{1}$$

$$\text{liquid:} \qquad \frac{\partial T}{\partial t} + \nabla\cdot(\mathbf{u}\,T) = Ma^{-1}\,\nabla\cdot\nabla\,T \tag{2}$$

$$\frac{\partial \omega}{\partial t} - \nabla\times(\mathbf{u}\times\omega) = -Re^{-1}\,\nabla\times\nabla\times\omega \tag{3}$$

$$\omega = \nabla\times\nabla\times\left(\frac{\Psi}{r}\,\hat{\theta}\right) \tag{4}$$

$$\text{where} \qquad \mathbf{u} = \nabla\times\left(\frac{\Psi}{r}\,\hat{\theta}\right) = -\frac{1}{r}\frac{\partial\Psi}{\partial z}\,\hat{\mathbf{r}} + \frac{1}{r}\frac{\partial\Psi}{\partial r}\,\hat{\mathbf{z}} \tag{5}$$

with the boundary conditions:

$$\text{solid surface } z=0 \quad : \quad \frac{\partial T}{\partial z} = 0 \tag{6}$$

$$\text{liquid surface } z=0 \quad : \quad \frac{\partial T}{\partial z} = -q(r) \tag{7}$$

$$\Psi = 0 \tag{8}$$

$$\omega = \frac{\partial T}{\partial r}\,\hat{\theta} \tag{9}$$

$$\text{axis } r=0 \quad : \quad \frac{\partial T}{\partial r} = 0 \tag{10}$$

$$\Psi = 0 \tag{11}$$

$$\omega = \mathbf{0} \tag{12}$$

$$\text{far away } r,z\to\infty \quad : \quad \frac{\partial T}{\partial R}\to -\frac{T}{R} \quad \left(\text{where } R\equiv\sqrt{r^2+z^2}\right) \tag{13}$$

$$\text{interface } r=f(z,t) \quad : \quad T=1 \tag{14}$$

$$\Psi=\frac{\partial \Psi}{\partial n}=0 \tag{15}$$

$$V_n=\alpha^{-1}\left[\left(\frac{\partial T}{\partial n}\right)_s-\left(\frac{\partial T}{\partial n}\right)_l\right] \tag{16}$$

Here T is temperature, t is time, $\mathbf{u}$ is the velocity vector with components u and v in the r and z directions (cylindrical coordinates), ω is the vorticity vector (having only one component, in the $\hat{\theta}$ direction), Ψ is the axisymmetric stream function, $q(r)$ is the imposed surface heat flux (large at $r=0$, falling off to zero at some small value of r, such that $\int_0^\infty q(r)\,r\,dr=1$), $r=f(z,t)$ gives the position of the solid-liquid interface, and V_n is the normal velocity of the phase-change interfacewhere n refers to the direction normal to the interface (outward).

The main dimensionless parameters are the Marangoni number $Ma\equiv u_s d/\kappa=\gamma Q/\mu k\kappa$ and the Reynolds number $Re\equiv u_s d/\nu$. Their ratio gives the Prandtl number: $Pr\equiv\nu/\kappa=Ma/Re$. The other dimensionless parameter is the ratio of the phase-change and convective time scales, $\alpha\equiv t_p/t_c=\gamma QL/\nu k^2\Delta T$, and so plays no role in the steady-state solution where $V_n\to 0$. Here $u_s\equiv\gamma\,\Delta T/\mu$ is the velocity scale, $d\equiv Q/k\Delta T$ is the diffusive length scale, κ is thermal diffusivity, γ (assumed constant and positive) is the negative of the derivative of the surface tension with respect to temperature, Q is the total heat flux input, μ is viscosity, k is thermal conductivity, ν is kinematic viscosity, $\Delta T\equiv T_m-T_c$ is the difference between the melting temperature and the cold temperature far away, and L is the latent heat of fusion.

3 NUMERICAL METHODS

For computational purposes, the idealized problem of an unbounded solid was truncated to a finite domain in cylindrical coordinates. The boundary condition on this artificial boundary is that the temperature should decay in the same way as the conduction solution for the point source, that is,

$$\frac{\partial T}{\partial R}=-\frac{T}{R} \tag{17}$$

where $R=\sqrt{r^2+z^2}$ is the spherical coordinate. This asymptotic matching condition is reasonable (for several diffusion lengths away from the pool) and is far less restrictive than imposing the Dirichlet condition ($T=0$) on the outer boundary.

To calculate the steady state for various values of Ma and Pr, the time-dependent equations are stepped in time with fully implicit steps, for the advantages of absolute stability and large time steps. Then at each new time, an elliptic problem must be solved. For this, multilevel methods are used, based on a uniform grid in the (r,z) quarter-plane and the Fast Adaptive Composite (FAC) grid approach to ensure resolution of all small-scale local details. At the solid-liquid interface, each grid has irregular elements to fit the interface. At each time step, the position of the interface is adjusted based on the normal velocity V from (16). (Note that the dimensionless parameter α in (16) can be adjusted to control how quickly the interface changes.) The difference equations on the grid were developed from the Finite Volume Element (FVE) method. This method combines the exact conservation of mass, momentum, and energy of the finite volume method, with the flexibility of the finite element method in handling complicated boundary conditions, irregular grids, etc. (See [3] for an introduction to FAC and FVE methods.) The resulting system of algebraic equations is solved by line relaxation at each level.

3.1 FVE APPROACH

The Finite Volume Element (FVE) approach to discretizing the system involves decomposing the domain in two ways: as the union of a set of elements, whose vertices compose the set of grid points on which the unknowns are defined; and as the union of a set of control volumes, one for each grid point (see Figure 2). The unknowns are interpolated over each element, based on the values at the grid points, giving a continuous representation over the whole domain. This representation is used to integrate the conservation equations over each control volume. Hence, each control volume gives three equations involving the three unknowns at

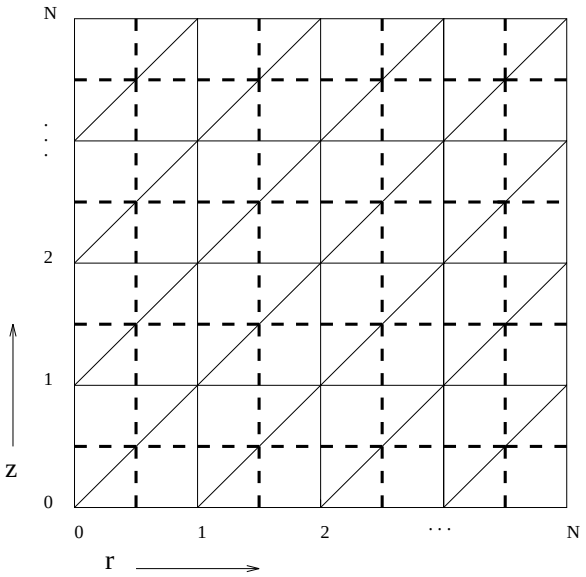

Figure 2: FVE Grid: the orientation of the triangular finite elements (thin lines) and the square finite volumes (thick dashed) are shown. On each triangular element, the variables are assumed linear between the three nodes. This allows consistent calculation of the gradients across the volume boundaries. Note that this is only a cross section in the (r, z) plane; the volumes extend in the θ direction to form rings.

the associated grid point, as well as the values at neighboring points. The resulting set of discrete equations for the finite element representation of the solution satisfies the conservation laws exactly over any volume made up of the union of control volumes, including the whole domain. (Actually, the boundary conditions may eliminate some of the control volumes.)

For this axisymmetric problem, each control volume is a toroidal prism, the result of taking a polygonal cross-section in the (r, z) plane and sweeping it all the way around in the θ direction (see Figure 3). Then integrating the convection-diffusion equation (2) over a control volume, interchanging time derivatives and spatial integrals, and applying the divergence theorem gives:

$$\frac{d}{dt} \iint_A T\, r\, dr\, dz + \oint_C \hat{\mathbf{n}} \cdot (\mathbf{u}\, T)\; r\, dl = Ma^{-1} \oint_C \hat{\mathbf{n}} \cdot \nabla T\, r\, dl \tag{18}$$

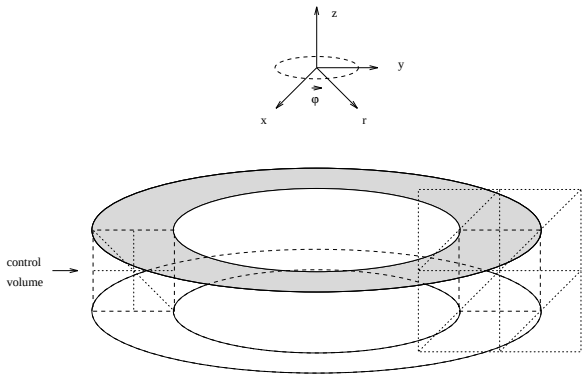

Figure 3: From axisymmetry, each control volume is a toroidal prism whose cross-section in the (r, z) plane is a square. Hence the size of the volume depends on radial position.

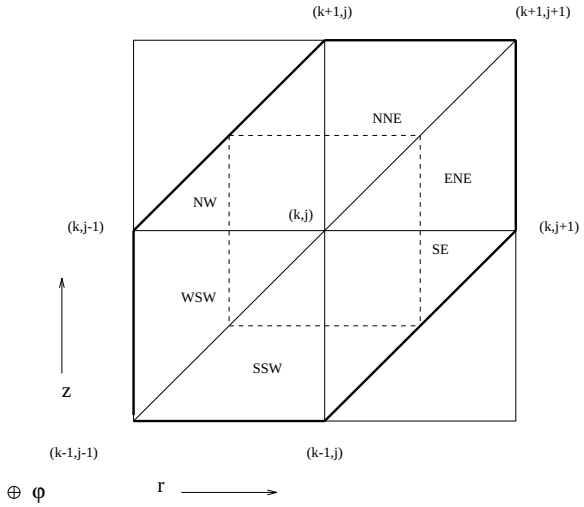

Figure 4: Each control volume involves six triangular elements, notated using compass directions.

where the 2π resulting from integration in θ has been factored out, A refers to the cross-sectional area (polygon) of the volume, C refers to the closed curve bounding that cross-section, and $\hat{\mathbf{n}}$ is the unit vector normal (outward) to C.

For the vorticity (3) and stream function equations (4), the control volume is a vorticity tube, and the appropriate integral is over the cross-sectional area A (with normal vector $\hat{\theta}$). Then applying Stokes' theorem gives:

$$\frac{d}{dt}\iint_A \omega\cdot\hat{\theta}\,dr\,dz - \oint_C \hat{\mathbf{t}}\cdot(\mathbf{u}\times\omega)\;dl \;=\; -Re^{-1}\oint_C \hat{\mathbf{t}}\cdot\nabla\times\omega\,dl \tag{19}$$

$$\oint_C \hat{\mathbf{t}}\cdot\mathbf{u}\,dl \;=\; \iint_A \omega\cdot\hat{\theta}\,dr\,dz \tag{20}$$

where $\hat{\mathbf{t}}$ is the unit vector tangent to C, in the positive θ sense.

Except near the phase-change interface, a uniform grid is applied with step size h in both the r and z directions (see Figure 2). (Portions of this grid may be subdivided into smaller uniform grids by the FAC method.) Each square of the grid is divided into two triangular elements by a diagonal (in the direction of increasing $r+z$), and linear interpolation is used over each triangular element. The control volume cross sections are squares of side h, centered on each grid point (except for half-squares at the boundaries and small quarter-squares at the corners).

Then in the integrated conservation equations (18, 19, 20), the area integrals are over six triangular regions (portions of the six elements), and the line integrals are over four line segments, each having halves in two different elements (see Figure 4). Then in terms of components, the integrated equations are

$$\begin{aligned}
&\frac{d}{dt}\iint_A T\,r\,dr\,dz \qquad\qquad (21)\\
&\quad + \int_N \frac{\partial\Psi}{\partial r}\,T\,dr + \int_E -\frac{\partial\Psi}{\partial z}\,T\,dz + \int_S -\frac{\partial\Psi}{\partial r}\,T\,dr + \int_W \frac{\partial\Psi}{\partial z}\,T\,dz\\
&\quad = Ma^{-1}\left(\int_N \frac{\partial T}{\partial z}\,r\,dr + \int_E \frac{\partial T}{\partial r}\,r\,dz + \int_S -\frac{\partial T}{\partial z}\,r\,dr + \int_W -\frac{\partial T}{\partial r}\,r\,dz\right)\\
&\frac{d}{dt}\iint_A \omega\,dr\,dz \qquad\qquad (22)\\
&\quad + \int_N \frac{\partial\Psi}{\partial r}\,\frac{\omega}{r}\,dr + \int_E -\frac{\partial\Psi}{\partial z}\,\frac{\omega}{r}\,dz + \int_S -\frac{\partial\Psi}{\partial r}\,\frac{\omega}{r}\,dr + \int_W \frac{\partial\Psi}{\partial z}\,\frac{\omega}{r}\,dz\\
&\quad = Re^{-1}\left(\int_N \frac{\partial\omega}{\partial z}\,dr + \int_E \frac{\partial(r\,\omega)}{\partial r}\,\frac{1}{r}\,dz + \int_S -\frac{\partial\omega}{\partial z}\,dr + \int_W -\frac{\partial(r\,\omega)}{\partial r}\,\frac{1}{r}\,dz\right)
\end{aligned}$$

$$-\iint_A \omega \, dr\, dz \quad = \quad \int_N \frac{\partial \Psi}{\partial z}\frac{1}{r}\, dr + \int_E \frac{\partial \Psi}{\partial r}\frac{1}{r}\, dz + \int_S -\frac{\partial \Psi}{\partial z}\frac{1}{r}\, dr + \int_W -\frac{\partial \Psi}{\partial r}\frac{1}{r}\, dz \tag{23}$$

where from here onward, ω refers to the one nonzero component of vorticity, and the labels N, E, S, and W refer to the four line segments of the line integrals by "compass direction" relative to the central node.

3.2 STENCIL CALCULATION WITH MAPLE

The calculation of the integrals and their combination to get the coefficients (stencils) for the discrete equations was done using *Maple* to minimize both labor and errors. Here is a brief summary of the methods used. (The worksheet "calcvort.ms" in the electronic supplement shows all the steps in calculating the vorticity and stream function equation stencils.)

Initially, my approach involved using subscripts $[i, j]$ to refer to particular points. But *Maple* (Release 3) had some bugs in trying to integrate expressions involving indexed names, so I switched to names concatenated with suffixes for the "compass direction" relative to the central point, then substituted into indexed form as the final step. (Unfortunately, I never eliminated the i, j arguments from the triangle interpolation functions, which now do not use them.)

To generate the linear interpolation functions over each triangle, the function `plane` takes three points and generates a function for the plane through those points, that is, the resulting function takes two variables and gives the interpolated (or extrapolated) value of the third.

```
> plane := proc(x1,y1,z1,x2,y2,z2,x3,y3,z3) local a,b,c,x,y;
> unapply(
>    subs(
>       solve({
>          a*x1+b*y1+c=z1,
>          a*x2+b*y2+c=z2,
>          a*x3+b*y3+c=z3},
>       {a,b,c}),
>    a*x+b*y+c),
> x,y );
> end:
```

Each stencil involves interpolation over six triangles in the (r, z) plane; the six triangle functions take a variable name (such as `omega` for vorticity) and return the corresponding interpolation function. For example, the "east-northeast" triangle uses `triene` (renotated for clarity):

```
> triene := (i,j,var) -> plane(rp,zp,var._p,rp+h,zp,var._e,rp+h,zp+h,var._ne):
```

Here the suffix "p" refers to the central point, at position (r_p, z_p), and h is the grid spacing. So `triene(omega)` returns the interpolation based on the nodal values $\omega_p, \omega_e, \omega_{ne}$.

The interpolations are used in evaluating the integrals. For example, to calculate the vorticity diffusion stencil (from the last set of terms in (22), with the coefficient Re^{-1}) involves derivatives of the interpolations with scaling in the radial coordinate r, integrated over the eight segments of the boundary:

```
> int( +(D[1](triene(i,j,omega))(re,z)+triene(i,j,omega)(re,z)/re), z=zp..zn) +
> int( +D[2](trinne(i,j,omega))(r,zn), r=rp..re) +
> int( +D[2](trinw(i,j,omega))(r,zn), r=rw..rp) +
> int( -(D[1](trinw(i,j,omega))(rw,z)+trinw(i,j,omega)(rw,z)/rw), z=zp..zn) +
> int( -(D[1](triwsw(i,j,omega))(rw,z)+triwsw(i,j,omega)(rw,z)/rw), z=zs..zp) +
> int( -D[2](trissw(i,j,omega))(r,zs), r=rw..rp) +
> int( -D[2](trise(i,j,omega))(r,zs), r=rp..re) +
> int( +(D[1](trise(i,j,omega))(re,z)+trise(i,j,omega)(re,z)/re), z=zs..zp) :
> diffv := simplify(");
```

where the definitions $r_w := r_p - h/2$, $r_e := r_p + h/2$, $z_s := z_p - h/2$, $z_n := z_p + h/2$ had been made previously.

Such a result still needs some massaging to get it into a useful form. The `varlist` function returns a list of the names of the nodal values of the given variable:

```
> varlist := (var) -> [var.(_sw,_s,_se,_w,_p,_e,_nw,_n,_ne)];
> vortlist := varlist(omega);
```

which can be used to collect terms to get the coefficient of each:

```
> collect(diffv,vortlist);
> diffv := map(simplify,");
```

Conversion into indexed notation is accomplished by the function `toindex`, which replaces the suffixed names of the specified variable:

```
> toindex := proc(expr,var) local n,m;
> subs(
>    zip( (x,y)->(x=y),
```

```
>       [var.(_sw,_s,_se,_w,_p,_e,_nw,_n,_ne)],
>       [seq(seq(var[i+n,j+m],n=-1..1),m=-1..1)]),
> expr );
> end:
```

This gives the output in the form

```
> toindex(diffv,omega);
```

$$-\frac{1}{4}\frac{\omega_{i-1,j-1}\,h}{2\,rp-h}+\frac{1}{4}\frac{\omega_{i,j-1}\,(8\,rp+5\,h)}{2\,rp+h}+\frac{1}{4}\frac{\omega_{i-1,j}\,(8\,rp-7\,h)}{2\,rp-h}-\frac{1}{2}\frac{(32\,rp^2-5\,h^2)\,\omega_{i,j}}{(2\,rp+h)\,(2\,rp-h)}$$
$$+\frac{1}{4}\frac{\omega_{i+1,j}\,(8\,rp+7\,h)}{2\,rp+h}+\frac{1}{4}\frac{\omega_{i,j+1}\,(8\,rp-5\,h)}{2\,rp-h}+\frac{1}{4}\frac{\omega_{i+1,j+1}\,h}{2\,rp+h}$$

Some further simplifications were made by hand, to more clearly show the effects of the radial scaling. Similar calculations were used for the other operators in the equations (and modified versions for the boundary conditions) to yield the stencils.

3.3 FVE STENCILS

Then at a typical grid point, the discrete equations (using stencil notation) become:

$$\frac{d}{dt}\frac{h^2}{24}\begin{pmatrix} & 2-\frac{5}{16}\epsilon & 1+\frac{5}{16}\epsilon \\ 2-\frac{11}{16}\epsilon & 14 & 2+\frac{11}{16}\epsilon \\ 1-\frac{5}{16}\epsilon & 2+\frac{5}{16}\epsilon & \end{pmatrix} T$$
$$+\frac{1}{8r}\begin{pmatrix} & & \begin{pmatrix} & & 1 \\ -2 & 1 & \end{pmatrix}\Psi & \begin{pmatrix} & -1 & \\ & & 1 \end{pmatrix}\Psi \\ & \begin{pmatrix} & 2 & \\ & -1 & \\ -1 & & \end{pmatrix}\Psi & \begin{pmatrix} & -1 & \\ 1 & & 1 \\ & -1 & \end{pmatrix}\Psi & \begin{pmatrix} & -1 & \\ & & -1 \\ & 2 & \end{pmatrix}\Psi \\ & \begin{pmatrix} 1 & & \\ & -1 & \end{pmatrix}\Psi & \begin{pmatrix} & 1 & -2 \\ 1 & & \end{pmatrix}\Psi & \end{pmatrix} T$$
$$= Ma^{-1}\begin{pmatrix} & 1 & \\ 1-\frac{1}{2}\epsilon & -4 & 1+\frac{1}{2}\epsilon \\ & 1 & \end{pmatrix} T \qquad (24)$$

$$\frac{d}{dt}\frac{h^2}{24}\begin{pmatrix} & 2 & 1 \\ 2 & 14 & 2 \\ 1 & 2 & \end{pmatrix}\omega$$
$$+\frac{1}{8r}\begin{pmatrix} & & \begin{pmatrix} & \frac{1}{2}\epsilon^+ & 1 \\ -2 & 1-\frac{1}{2}\epsilon^+ & \end{pmatrix} & \begin{pmatrix} -1 & \frac{1}{2}\epsilon^- \\ & 1^- \end{pmatrix} \\ \begin{pmatrix} & 2*1^+ & \\ \frac{1}{2}\epsilon^+ & -1-\epsilon^+ & \\ -1^+ & & \end{pmatrix} & [C]\Psi & \begin{pmatrix} & & -1^- \\ -1+\epsilon^- & -\frac{1}{2}\epsilon^- & \\ 2*1^- & & \end{pmatrix} \\ \begin{pmatrix} 1^+ & & \\ -\frac{1}{2}\epsilon^+ & -1 & \end{pmatrix} & \begin{pmatrix} & 1+\frac{1}{2}\epsilon^- & -2 \\ 1 & -\frac{1}{2}\epsilon^- & \end{pmatrix} & \end{pmatrix}\omega$$
$$= Re^{-1}\begin{pmatrix} & 1-\frac{1}{8}\epsilon^+ & \frac{1}{8}\epsilon^- \\ 1-\frac{3}{8}\epsilon^+ & -\left[4+\frac{3}{8}(\epsilon^+-\epsilon^-)\right] & 1+\frac{3}{8}\epsilon^- \\ -\frac{1}{8}\epsilon^+ & 1+\frac{1}{8}\epsilon^- & \end{pmatrix}\omega \qquad (25)$$

$$\begin{pmatrix} & 1 & \\ 1^+ & -[2+1^++1^-] & 1^- \\ & 1 & \end{pmatrix}\Psi = -\frac{rh^2}{24}\begin{pmatrix} & 2 & 1 \\ 2 & 14 & 2 \\ 1 & 2 & \end{pmatrix}\omega \qquad (26)$$

where $[C]\Psi \equiv \begin{pmatrix} & -1+\frac{1}{2}\epsilon^+ & \epsilon^- \\ 1+\epsilon^+ & -\epsilon^+ + \epsilon^- & 1-\epsilon^- \\ -\epsilon^+ & -1-\frac{1}{2}\epsilon^- & \end{pmatrix}\Psi$, $\epsilon \equiv h/r$, $\epsilon^+ \equiv \frac{\epsilon}{1-\epsilon/2}$, $\epsilon^- \equiv \frac{\epsilon}{1+\epsilon/2}$, $1^+ \equiv \frac{1}{1-\epsilon/2}$, $1^- \equiv \frac{1}{1+\epsilon/2}$, and r is the radial coordinate at the central point P. In the stencil notation, for example $\begin{pmatrix} a & b & c \\ d & e & f \\ g & h & i \end{pmatrix} T$, the entries in the matrix (a, $b \ldots$) are the coefficients of the values the unknown (T) at the corresponding points, where the center of the matrix corresponds to the current point P, and r, z are horizontal and vertical, respectively. Blank entries indicate zero coefficients, and a central Σ indicates the sum of all the other coefficients in the matrix. Note that in the nonlinear convective terms, each of the coefficients of T or ω is itself expressed as a stencil in Ψ (each centered at the same point P); to save space, the Ψ is left out of the vorticity convection stencil. Note that for those integrals in r with integrands containing a $1/r$, that factor was pulled outside the integral to avoid logarithms; the error introduced is of the same order as that due to the piecewise linear representation itself. Also, the heat equation was rescaled by $1/r$, and the stream function equation rescaled by r.

The radial dependence of the coefficients is a direct result of the axisymmetric geometry. This dependence makes the calculation somewhat more complicated than the corresponding two-dimensional problem. But far from the axis, where $r \gg h$ and hence $\epsilon \ll 1$, the equations approach the corresponding two-dimensional versions, facilitating comparison.

3.4 Discretized Boundary Conditions

Along the surface $z = 0$, each of the three boundary conditions for the three unknowns requires different treatment. The temperature at each grid point along the surface is determined by a heat balance over the corresponding control volume, with half-square cross section $(h \times h/2)$. The contribution of the surface to the convective flux integral is zero, since there is no velocity normal to the surface, and the contribution of the surface to the diffusive flux integral is given by the Neumann type boundary condition $\int q(r) r\, dr$. The resulting discrete equation is

$$\begin{aligned} \frac{d}{dt}\frac{h^2}{24} & \begin{pmatrix} & 2-\frac{5}{16}\epsilon & 1+\frac{5}{16}\epsilon \\ \frac{3}{2}-\frac{1}{2}\epsilon & 7+\frac{5}{16}\epsilon & \frac{1}{2}+\frac{3}{16}\epsilon \end{pmatrix} T \\ + \frac{1}{8r} & \begin{pmatrix} & & \begin{pmatrix} & 1 & \end{pmatrix}\Psi & \begin{pmatrix} & -1 & \end{pmatrix}\Psi \\ \begin{pmatrix} & 2 & \end{pmatrix}\Psi & \begin{pmatrix} & -1 & \end{pmatrix}\Psi & \begin{pmatrix} & & \end{pmatrix}\Psi & \begin{pmatrix} & -1 & \end{pmatrix}\Psi \end{pmatrix} T \\ = \; Ma^{-1} & \begin{pmatrix} \frac{1}{2}-\frac{1}{4}\epsilon & 1 & \frac{1}{2}+\frac{1}{4}\epsilon \\ & -2 & \end{pmatrix} T + \frac{1}{r\,Ma}\int_{r-h/2}^{r+h/2} q(r) r\, dr \end{aligned} \tag{27}$$

Here we specify the heat flux as a symmetric function of r that decays smoothly to zero at some finite radius ρ_{max}, while satisfying $\int_0^\infty q(r) r\, dr = 1$:

$$q(r) \equiv \begin{cases} \frac{6}{\rho_{max}^2}\left[1-\left(\frac{r}{\rho_{max}}\right)^2\right]^2, & r \le \rho_{max} \\ 0, & r > \rho_{max} \end{cases} \tag{28}$$

For the calculations, we use $\rho_{max} = \frac{1}{4}$.

The thermocapillary stress condition at the surface specifies the vorticity: $\omega = \frac{\partial T}{\partial r}$. However, because of the linear interpolation between grid points, $\frac{\partial T}{\partial r}$ is not well defined at grid points on the surface. Hence, for the surface only, the vorticity is specified at half-grid points (i.e., $r = (i+\frac{1}{2})h$), and triangular finite elements are formed with neighboring points. This keeps the discretization of this important condition at

the same order of accuracy as the other equations, but entails special treatment of the grid points next to the surface. The surface is also a streamline, where $\Psi = 0$ (Dirichlet condition). Using that fact and these special surface vorticity elements gives the following flow equations for points by the surface (a distance h from the surface):

$$
\begin{aligned}
&\frac{d}{dt}\frac{h^2}{24}\begin{pmatrix} \frac{19}{8} & 2 & 1 \\ & 14\frac{1}{4} & \frac{11}{8} \end{pmatrix}\omega + \frac{d}{dt}\frac{h}{16}\begin{pmatrix} & & \\ -1 & & 1 \end{pmatrix} T \\
&+ \frac{1}{8r}\begin{pmatrix} & & \begin{pmatrix} & \frac{1}{2}+\frac{3}{4}\epsilon^+\epsilon^+ & 1 \\ -2 & 1-\frac{1}{2}\epsilon^+ & \end{pmatrix} & \begin{pmatrix} -1 & \frac{1}{2}\epsilon^- \\ & 1^- & \end{pmatrix} \\ \begin{pmatrix} \frac{1}{2}+\frac{3}{4}\epsilon^+ & 2*1^+ \\ & -1-\epsilon^+ \end{pmatrix} & & [C]\Psi & \begin{pmatrix} & -1^- \\ -\frac{5}{4}+\frac{3}{4}\epsilon^- & \frac{3}{4}-\frac{1}{2}\epsilon^- \end{pmatrix} \end{pmatrix}\omega \\
&+ \frac{1}{8rh}\begin{pmatrix} & & \\ \begin{pmatrix} -1^+ & -\frac{1}{4} & \frac{1}{4} \end{pmatrix} & \begin{pmatrix} 1^+ & -\frac{1}{2}-\frac{1}{2}\epsilon^+ & \frac{3}{2} \end{pmatrix} & \begin{pmatrix} \frac{3}{4}+\frac{1}{2}\epsilon^+ & -\frac{7}{4} \end{pmatrix} \end{pmatrix} T \\
&= Re^{-1}\begin{pmatrix} \frac{7}{8}-\frac{7}{16}\epsilon^+ & 1-\frac{1}{8}\epsilon^+ - \left[\frac{15}{4}+\frac{5}{16}\epsilon^+ - \frac{7}{16}\epsilon^-\right] & \frac{1}{8}\epsilon^- \\ & & \frac{7}{8}+\frac{5}{16}\epsilon^- \end{pmatrix}\omega \\
&+ Re^{-1}\frac{1}{h}\begin{pmatrix} & & \\ -\frac{1}{2}+\frac{1}{8}\epsilon^+ & -\frac{1}{8}\epsilon^+ - \frac{1}{8}\epsilon^- & \frac{1}{2}+\frac{1}{8}\epsilon^- \end{pmatrix} T \qquad (29) \\
&\begin{pmatrix} & 1 & \\ 1^+ & -[2+1^++1^-] & 1^- \\ & & \end{pmatrix}\Psi \\
&= \frac{rh^2}{24}\begin{pmatrix} \frac{19}{8} & 2 & 1 \\ & 14\frac{1}{4} & \frac{11}{8} \end{pmatrix}\omega + \frac{rh}{16}\begin{pmatrix} & & \\ -1 & & 1 \end{pmatrix} T \qquad (30)
\end{aligned}
$$

where $[C]\Psi \equiv \begin{pmatrix} & -1+\frac{1}{2}\epsilon^+ & \epsilon^- \\ \frac{1}{2}+\frac{3}{4}\epsilon^+ & 1-\frac{1}{2}\epsilon^+ + \frac{3}{4}\epsilon^- & \frac{1}{4}-\epsilon^- \end{pmatrix}\Psi$.

Along the z axis, symmetry requires that there is no heat flux across the axis, nor flow, nor shear stress, so both Ψ and ω are zero there. Then for points on the axis, the discrete heat balance over the cylindrical control volumes (half square cross section $h/2 \times h$) gives:

$$
\begin{aligned}
&\frac{d}{dt}\frac{h^2}{24}\begin{pmatrix} \frac{1}{4} & \frac{5}{4} \\ \frac{25}{4} & \frac{11}{4} \\ \frac{6}{4} & \end{pmatrix} T \\
&+\frac{1}{2h}\begin{pmatrix} \begin{pmatrix} & 1 \end{pmatrix}\Psi & \begin{pmatrix} & 1 \end{pmatrix}\Psi \\ \begin{pmatrix} & 1 \end{pmatrix}\Psi & \begin{pmatrix} & -1 \end{pmatrix}\Psi \\ \begin{pmatrix} & -2 \end{pmatrix}\Psi & \end{pmatrix} T
\end{aligned}
$$

$$-Ma^{-1}\begin{pmatrix} & \frac{1}{2} & \\ & -3 & 2 \\ & \frac{1}{2} & \end{pmatrix} T \;=\; 0 \tag{31}$$

where the equation was scaled using the average $\bar{r} = h/4$. The homogeneous Dirichlet conditions on Ψ and ω apply to points on the axis, and for grid points neighboring the axis, the usual stencils apply; no special treatment is necessary.

The temperature at the grid point at the origin is determined by a small control volume (quarter square cross section $h/2 \times h/2$) with specified surface heat flux and no flux (nor convection) through the axis:

$$\frac{d}{dt}\frac{h^2}{24}\begin{pmatrix} \frac{1}{4} & \frac{5}{4} \\ \frac{15}{4} & \frac{3}{4} \end{pmatrix} T$$

$$+\frac{1}{2h}\begin{pmatrix} \begin{pmatrix} & 1 \\ & \end{pmatrix}\Psi & \\ & \begin{pmatrix} & -1 \\ & \end{pmatrix}\Psi \end{pmatrix} T$$

$$-Ma^{-1}\begin{pmatrix} \frac{1}{2} & \\ -\frac{3}{2} & 1 \end{pmatrix} T \;=\; Ma^{-1}\frac{4}{h}\int_0^{h/2} q(r) r\, dr \tag{32}$$

Again, at the origin, both Ψ and ω are zero (note the two boundary conditions on vorticity are consistent at this point, due to the symmetry). Hence, the usual surface flow equations apply to the grid point next to the origin.

At the far boundaries of the computational domain, the boundary condition on the heat diffusion equation in the solid is that it decays in the same way as the spherically symmetric solution for a point source:

$$\nabla T = \frac{\partial T}{\partial R}\hat{\mathbf{R}} = -\frac{T}{R}\hat{\mathbf{R}} = -T\frac{r}{R^2}\hat{\mathbf{r}} - T\frac{z}{R^2}\hat{\mathbf{z}} \tag{33}$$

where $R \equiv \sqrt{r^2 + z^2}$. This allow the heat flux across the artificial boundary to be computed in terms of the temperature there, a Robin type boundary condition. Below we give the discrete equations for the two edges (half-square volumes) and three corners (quarter-square volumes) where this boundary condition is applied.

At the edge where r is at its maximum:

$$\frac{d}{dt}\frac{h^2}{24}\begin{pmatrix} & & \frac{3}{2} - \frac{3}{8}\epsilon \\ 2 - \frac{11}{16}\epsilon & 7 - \frac{25}{16}\epsilon & \\ 1 - \frac{5}{16}\epsilon & \frac{1}{2} - \frac{1}{16}\epsilon & \end{pmatrix} T$$

$$-Ma^{-1}\begin{pmatrix} & & \frac{1}{2} - \frac{1}{8}\epsilon - \frac{1}{8}\rho \\ 1 - \frac{1}{2}\epsilon & -2 + \frac{3}{4}\epsilon - \frac{3}{4}\rho & \\ & \frac{1}{2} - \frac{1}{8}\epsilon - \frac{1}{8}\rho & \end{pmatrix} T \;=\; 0 \tag{34}$$

where $\rho \equiv hr/(r^2 + z^2)$.

At the edge where z is at its maximum:

$$\frac{d}{dt}\frac{h^2}{24}\begin{pmatrix} \frac{1}{2} - \frac{3}{16}\epsilon & 7 - \frac{5}{16}\epsilon & \frac{3}{2} + \frac{1}{2}\epsilon) \\ 1 - \frac{5}{16}\epsilon & 2 + \frac{5}{16}\epsilon & \end{pmatrix} T$$

$$-Ma^{-1}\begin{pmatrix} \frac{1}{2} - \frac{1}{4}\epsilon - \frac{1}{8}(1 - \frac{1}{3}\epsilon)\zeta & -2 - \frac{3}{4}\zeta & \frac{1}{2} + \frac{1}{4}\epsilon - \frac{1}{8}(1 + \frac{1}{3}\epsilon)\zeta \\ & 1 & \end{pmatrix} T \;=\; 0 \tag{35}$$

where $\zeta \equiv hz/(r^2 + z^2)$.

At the corner where both r and z are maximum:

$$\frac{d}{dt}\frac{h^2}{24}\begin{pmatrix} \frac{1}{2}-\frac{3}{16}\epsilon & 4-\frac{15}{16}\epsilon \\ 1-\frac{5}{16}\epsilon & \frac{1}{2}-\frac{1}{16}\epsilon \end{pmatrix} T$$

$$-Ma^{-1}\begin{pmatrix} \frac{1}{2}-\frac{1}{4}\epsilon-\frac{1}{8}(1-\frac{1}{3}\epsilon) & -1+\frac{3}{8}\epsilon-\frac{3}{8}[\rho+(1-\frac{2}{9}\epsilon)\zeta] \\ & \frac{1}{2}-\frac{1}{8}\epsilon-\frac{1}{8}\rho \end{pmatrix} T = 0 \quad (36)$$

At the corner where $r = 0$ and z is maximum:

$$\frac{d}{dt}\frac{h^2}{24}\begin{pmatrix} \frac{5}{2} & 2 \\ \frac{3}{2} & \end{pmatrix} T$$

$$-Ma^{-1}\begin{pmatrix} -\frac{3}{2}-\frac{1}{3}\zeta & 1-\frac{1}{6}\zeta \\ \frac{1}{2} & \end{pmatrix} T = 0 \quad (37)$$

At the corner where r is maximum and $z = 0$:

$$\frac{d}{dt}\frac{h^2}{24}\begin{pmatrix} & \frac{3}{2}-\frac{3}{8}\epsilon \\ \frac{3}{2}-\frac{1}{2}\epsilon & 3-\frac{5}{8}\epsilon \end{pmatrix} T$$

$$-Ma^{-1}\begin{pmatrix} & \frac{1}{2}-\frac{1}{8}\epsilon-\frac{1}{8}\rho \\ \frac{1}{2}-\frac{1}{4}\epsilon & -1+\frac{3}{8}\epsilon-\frac{3}{8}\rho \end{pmatrix} T = 0 \quad (38)$$

3.5 Tracking the Phase-Change Interface

One of the biggest challenges in models of phase change is the tracking over time of the position of the two-phase interface. As one of the main goals of the current research is the examination of the effects of thermocapillary convection on the interface shape, great care is necessary in accurately modeling the geometry and dynamics of the phase change process. However, the details of how the grid is modified near the interface, and the derivation of appropriate stencils, will not be described here. Suffice it to say that *Maple* was again essential in evaluating the integrals to find the coefficients.

4 Results

This is work in progress. To date, the basic equations have been solved assuming the pool is a unit cylinder. In the conductive limit, the results match the solution caclulated by the Green's function method, giving confidence in the method. Implementation of the moving phase-change boundary is underway.

The FVE approach in this problem satisfies the conservation equations exactly while using continuous representations of the unknowns. The cost for these desirable features it that calculation of the coefficients is complicated. *Maple* made this approach much more feasible.

ACKNOWLEDGMENTS

This work was supported by the Office of Naval Research, Materials Division (contract N0001492WR24009).

References

[1] D. Canright. Thermocapillary flow near a cold wall. *Phys. Fluids*, 6:1415–1424, 1994.

[2] M. M. Chen. Thermocapillary convection in materials processing. In S. K. Samanta, R. Komandiri, R. McMeeking, M. M. Chen, and A. Tseng, editors, *Interdisciplinary Issues in Materials Processing and Manufacturing*, pages 541–557. ASME, 1987.

[3] Stephen F. McCormick. *Multilevel Adaptive Methods for Partial Differential Equations.* Society for Industrial and Applied Mathematics, Philadelphia, 1989.